Amendable decisions in living systems

Izaak Neri[1,2*†], Simone Pigolotti[3*†]

[1]Department of Mathematics, King's College London, Strand, London, WC2R 2LS, UK.

[2]Theoretical Sciences Visiting Program (TSVP), Okinawa Institute of Science and Technology Graduate University, Onna, 904-0495, Japan.

[3]Biological Complexity Unit, Okinawa Institute of Science and Technology Graduate University, Onna, 904-0495, Japan.

*Joint corresponding authors. Email: izaak.neri@kcl.ac.uk, simone.pigolotti@oist.jp .

†These authors contributed equally to this work.

A distinct feature of living systems is their capacity to take decisions based on uncertain environmental signals. Examples span from the microscopic scale of cell differentiation guided by the concentration of a morphogen, to complex choices made by animals and humans. The current paradigm in decision theory assumes that decisions, once taken, cannot be revoked. However, living systems often amend their decisions if new evidence favors an alternative hypothesis. In this paper, we characterize the optimal strategy for such amendable decisions. We find that, unlike irrevocable decisions, optimal amendable decisions can be made in a finite average time with zero error probability. Our theory successfully predicts the outcome of a visual experiment involving human participants and the accuracy of cell-fate decisions in early development. Our study reveals that amendments lead to a substantial advantage in decision-making, that is likely to be widely exploited by living beings.

Living systems are able to make appropriate decisions based on signals received by their environment. Examples can be found in animal behavior (*1*), such as in mate choice (*2*), foraging (*3, 4*), and prey and predator detection (*5*). Performance in decision tasks has been extensively tested in laboratory experiments (*1, 4, 6, 7*). Being able to decide rapidly and appropriately is often a matter of life and death. For this reason, living systems are often argued to employ optimal decision strategies (*8–10*). We focus on decision processes in which living observers have in mind different, mutually exclusive hypotheses about their environment. They then accumulate information about the environment, and store them in an internal representation called the evidence. At some point in time, they decide, based on the evidence, which of the hypotheses they believe to be correct.

The literature on biological decision making has predominantly focused on decisions that cannot be revoked. In this case, the optimal decision strategy has been identified by Wald as the sequential probability ratio test (*11–13*). In this test, the evidence is constructed as the logarithm of the likelihood ratio of the two hypotheses, and a decision is taken as soon as the evidence reaches either

a positive or a negative threshold. The sequential probability ratio test can be used as a normative model to rationalize fast decisions by animals and humans receiving perceptual stimuli (*14*). The optimal decision strategy is characterized by speed-accuracy tradeoffs (*1, 15, 16*). For example, the average decision time increases as the similarity between the hypotheses is increased. Additionally, the average decision time increases as the error probability, i.e., the probability of committing for the wrong hypothesis, is decreased. Speed-accuracy tradeoffs have been confirmed in behavioral experiments on olfactory (*7*), visual (*3, 6*), and tactile (*17*) tasks performed by animals (*3, 7, 17, 18*) and humans (*6*); see (*1, 16*) for reviews.

Certain fast and accurate cellular processes, such as the expression of genes in response to morphogene signals (*8, 19–22*), T-cell activation in response to foreign ligands (*23*), and stem cell differentiation (*24*) can be conceptualized as decisions as well (*25–27*). The sequential probability ratio test has also been applied to this kind of decisions (*22, 27, 28*). A classic example of a cell-fate decision is the expression of the gap gene Hunchback by nuclei in the embryo of the fruit fly *Drosophila melanogaster* in response to the morphogen Bicoid (*8, 26*). These nuclei decide whether to express Hunchback in about 5-10 minutes, much faster (*8, 29*) than the estimated lower limit of about 2 hours set by the Berg-Purcell bound (*30*). This discrepancy can be resolved using an irrevocable decision model (*22*), provided that Bicoid binds cooperatively to the Hunchback promoter.

Irrevocable decisions are often unnatural for living beings. Perceptual studies have shown that humans often change their mind after having perceived a stimulus and taken a decision, thereby reducing their error probability (*31–33*). It is also debatable whether cellular decisions are mostly irrevocable. For example, in vivo imaging of the Bicoid-Hunchback system show that Hunchback can switch its expression level several times in a nuclear cycle (*34*). Direct measurements of Hunchback transcription rates support an alternate on-off gene activity as well (*35*). More broadly, subcellular regulatory systems responsible of decisions are likely to gradually commit to a particular outcome, rather than undergo a sudden irreversible transition (*36–38*).

In this paper, we present a theory for decision processes in which, after decisions, observers maintain their right to change their mind, should additional evidence overwhelmingly favor the alternative hypothesis. We identify the optimal strategy in this scenario. In stark contrast with irrevocable decisions, this optimal amendable strategy is characterized by a vanishing error probability in a finite average decision time. We apply our theory to a human perception study, finding support for our theoretical predictions. We also propose an amendable decision model for the Bicoid-Hunchback system. This model successfully predicts experimental decision statistics without adjustable parameters, corroborating the hypothesis that cell-fate decisions in this system are amendable and operate in a nearly optimal way.

Results

Irrevocable versus amendable decisions

We focus on decisions entailing two different hypotheses, + and −, on a certain phenomenon. An observer acquires information about this phenomenon by perceiving a time-dependent signal $X(t)$, see Fig. 1A. This signal is noisy and its statistics depend on which of the two hypotheses is true. The observer monitors the signal and stores the information contained in it into a time-dependent

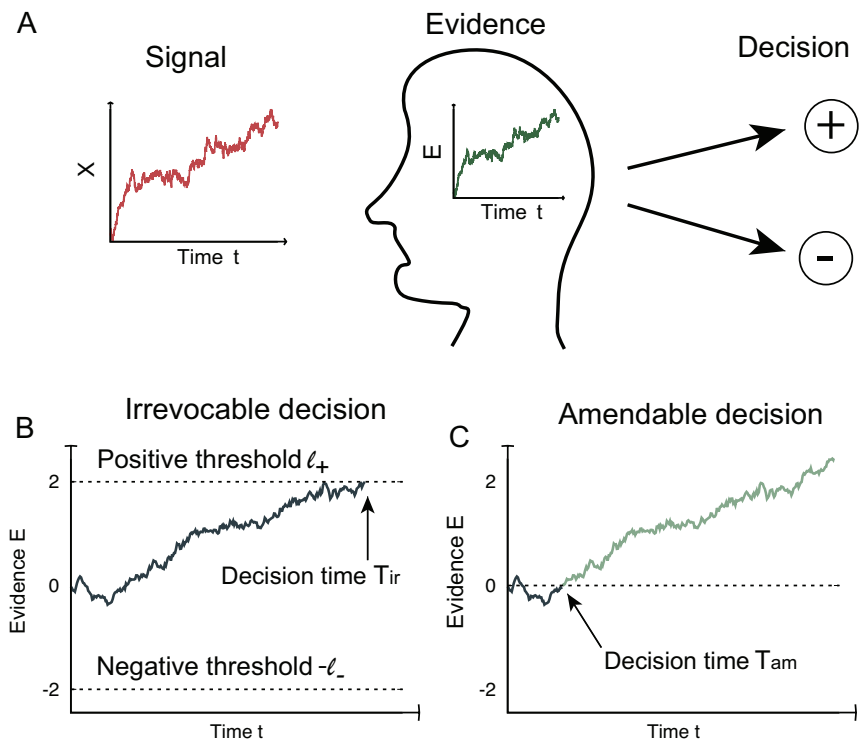

Figure 1: (A) Biological decision making. An environmental signal is observed by a living systems that stores the information contained in it in a process called the evidence. After having accumulated enough information, the observer makes a binary decision. (B) Irrevocable decision making. The observer commits to the + or - hypothesis as soon as the evidence crosses a positive or negative threshold, respectively. This commitment is irreversible. (C) Amendable decision making. In this case, the observer is in favor of the + or − hypothesis whenever $E(t)$ is greater or smaller than zero, respectively. A final decision time can be identified a posteriori as the moment when the evidence process crosses zero for the last time.

variable $E(t)$, called the evidence. This variable is constructed so that positive and negative values of E represent accumulated evidence supporting hypotheses + and −, respectively. The decision is a binary variable $D \in (+, -)$ that depends on the evidence and is considered correct if it matches the hypothesis.

Irrevocable and amendable processes differ in the nature of decisions. In an irrevocable decision, the observer commits to the hypothesis + (or −) as soon as the collected evidence crosses either a positive threshold ℓ_+ or a negative threshold $-\ell_-$, see Fig. 1B. This commitment is final. This idea is at the basis of Wald's sequential test (*11, 12*), in which the evidence is constructed as the logarithm of the likelihood ratio of the two hypotheses. The decision time $T_{\rm ir}$ is the time at which either of the thresholds is crossed for the first time. Properties of irrevocable decision processes can be calculated using the theory of first-passage times (*39*). Choosing larger thresholds amounts to safer decisions, i.e., a lower probability of committing to the wrong hypothesis. However, this comes at a cost of a longer decision time.

In an amendable decision process, observers can alter their choice, so that their decision is only tentative at any time during the observation. We call $d(t) \in (+, -)$ the tentative decision at time t. The natural strategy is to set $d(t)$ equal to the sign of $E(t)$. In practice, the evidence $E(t)$ can change sign several times, leading to multiple amendments to the tentative decision. However, even if the available time is unlimited, after a certain moment the accumulated evidence may be so overwhelming that the observer will never change opinion again. Alternatively, one could consider scenarios in which observers have a finite available time $t_{\rm f}$ to reach a decision. We define the final decision D as the large-time limit of $d(t)$ in the infinite-time case, or as $d(t_{\rm f})$ in the finite-time case. We also identify a posteriori a decision time $T_{\rm am}$ as the time when the evidence process crosses zero for the last time, see Fig. 1C.

Error-free amendable decisions in the drift-diffusion model

We consider signals whose statistics are described by a drift-diffusion model

$$\frac{dX}{dt} = \mu_\pm + \sigma\, \xi(t)\,, \tag{1}$$

where μ_+ and μ_- are the drift coefficients corresponding to the two hypotheses and $\xi(t)$ is white noise. Without loss of generality, we assume $\mu_+ > \mu_-$. We express the dynamics of the evidence process by

$$\frac{dE}{dt} = \pm\gamma + \xi(t) \tag{2}$$

where the plus/minus sign in the right hand side depends on which of the two hypotheses hold, and γ is the average rate of acquisition of evidence (see Methods). In (2), we have set the amplitude of the noise equal to one by an appropriate choice of the units of E. In (2), changing hypothesis simply changes the sign of the drift term. This assumption is justified when the observation process is similarly symmetric, i.e., when $\mu_- = -\mu_+$. Additionally, the evidence process presents this symmetry if it is optimal, even if the underlying observation process is not symmetric (see SI, Section 1). The more general case of a non-symmetric evidence process is also discussed in SI (Section 2).

For an irrevocable decision based on the Wald test, the optimal choice of evidence is given by the logarithm of the likelihood ratio, $E(t) \propto \ln P(X(t)|+)/P(X(t)|-)$. Here, $P(X(t)|+)$ and

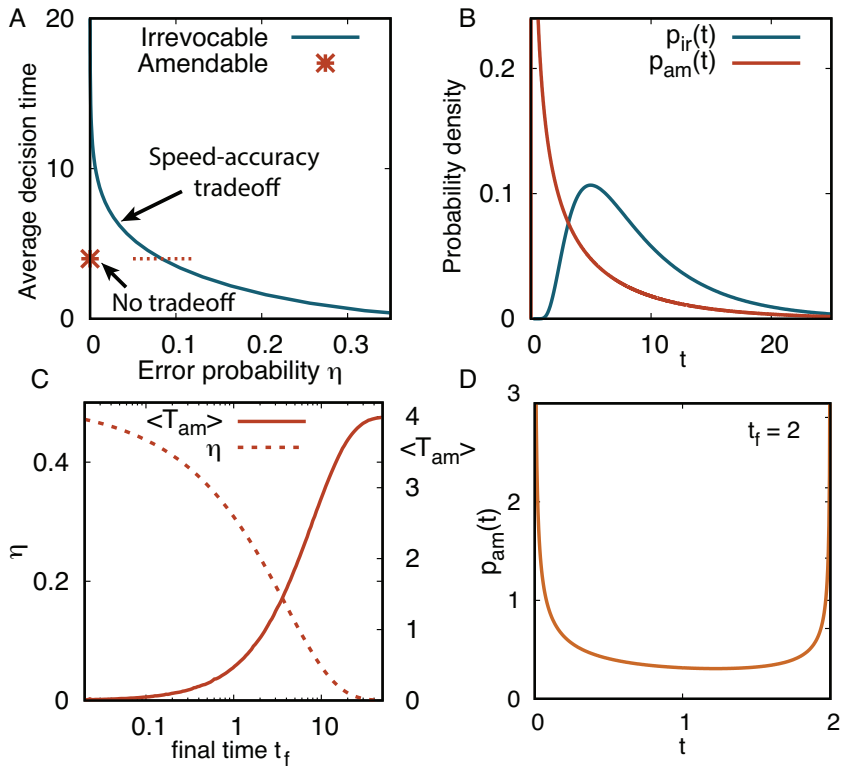

Figure 2: Optimal amendable and irrevocable decisions for the drift-diffusion process. The evidence process is governed by (2) with $\gamma = \gamma_{\rm opt} = 1/(2\sqrt{\tau})$ and units of time are such that $\tau = 1$. (A) Comparison of average decision times. In the irrevocable case, the decision time depends on the error probability η, while amendable decisions are always error-free ($\eta = 0$). Irrevocable decisions are faster for $\eta < \eta_c \approx 0.083$. (B) Decision time distributions for amendable and irrevocable decisions for infinitely large observation time $t_{\rm f}$. In the irrevocable case, we have set $\eta = 0.01$. (C) Average decision time and error probability for a finite observation time, $t \in [0, t_{\rm f}]$, and for amendable decisions. (D) Distribution of amendable decision times for a finite observation time.

$P(X(t)|+)$ are the probability distributions of $X(t)$ given the positive and negative hypothesis, respectively. This choice is optimal in the sense of minimizing the average irrevocable decision time at a given error probability (see Ref. (*40*) and SI, Section 1). The optimal evidence obeys (2) with $\gamma = \gamma_{\rm opt} = 1/(2\sqrt{\tau})$, where we have introduced the characteristic time $\tau = \sigma^2/(\mu_+ - \mu_-)^2$, see SI, Section 1. The initial condition depends on the initial prior on the two hypotheses. Throughout this paper, we shall assume that the two hypotheses are equally likely, so that the optimal initial condition is $E(0) = 0$. We focus on case of symmetric barriers $\ell_+ = -\ell_- = \ell$, where the probabilities of false positives and false negatives are equal.

We find that the log-likelihood ratio also constitutes the optimal choice of evidence in the amendable case (see SI, Section 1). This key result depends on assuming a homogeneous prior, i.e. on assuming that the two hypotheses are a priori equally likely and that the observer is aware of that. For an unequal prior, the likelihood ratio is not necessarily optimal (see SI, Section 3).

We compare the average optimal decision time in the two setups, see Fig. 2A. In the irrevocable

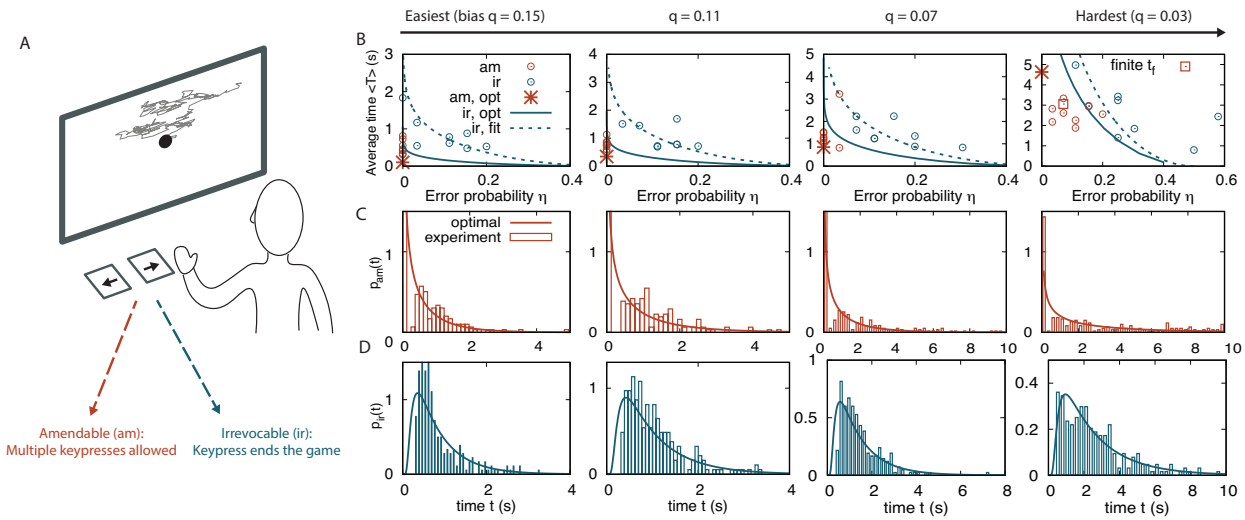

Figure 3: Amendable versus irreversible decisions in a visual perception experiment. (A) Sketch of the experiment. (B) Speed-error tradeoffs for the four game difficulties. The game difficulty is determined by the bias parameter q (see Methods). Circles represent the error probabilities and average decision times for each individual player. In the irrevocable cases, average decision times and error probabilities are characterized by a tradeoff (Pearson correlation coefficients among participants $r = (-0.68, -0.48, -0.61, -0.61)$ from easiest to hardest). The star and the continuous line mark the optimal strategies in the amendable and irrevocable cases, respectively (see Fig. 2A). In the optimal case, the parameter γ_{opt} is computed from the drift and diffusion of the moving dot (see Methods). The dashed lines represent the irrevocable strategy associated with a fitted evidence rate γ (see Methods). For $q = 0.03$, the square marks the optimal finite-time amendable strategy (see Methods). For all the other game difficulties, the finite-time amendable strategy is practically indistinguishable from the infinite-time one, and thus decisions are made with negligible error probability. (C) Empirical distributions of the amendable decision time, $p_{\text{am}}(t)$, compared with the theoretical optimal distribution given by (3). (D) Empirical distributions of the irrevocable decision time, $p_{\text{ir}}(t)$, compared with the optimal distribution estimated from the empirical error probability (see Methods).

case, the average decision time depends on the choice of the thresholds, and thus on how the observer trades off speed and error probability. In particular, for small error probability η, the average decision time scales as $\langle T_{\text{ir}} \rangle \sim -\log(\eta)$. In contrast, amendable decisions are free of errors ($\eta = 0$) and are reached in a finite average decision time $\langle T_{\text{am}} \rangle = 4\tau$. Amendable decisions are faster than irreversible decisions on average, unless the observer is willing to accept an error probability larger than a critical value $\eta_c \approx 0.08$, see Fig. 2A. While the distribution $p_{\text{ir}}(t)$ of irrevocable decision time presents a peak at an intermediate time, under our conditions of equal priors, the distribution of amendable decision times

$$p_{\text{am}}(t) = \frac{1}{\sqrt{8\pi t \tau}} \exp\left(-\frac{t}{8\tau}\right) \tag{3}$$

decreases monotonically, see Fig. 2B.

So far, we have considered cases in which the time available to the observer is unlimited. However, in practical situations, the observer might be forced to make a call within a certain maximum

time t_{f}. In such settings, amendable decisions are characterized by a finite error probability, see Fig. 2C and Methods. For small t_{f}, the distribution of decision times presents a bimodal shape, see Fig. 2D and Methods. The second peak close to t_{f} is due to the conditioning of a decision before the maximum time: a transition via the state $E = 0$ has an increased chance of being the last one if it occurs right before t_f (see Methods).

Amendable vs. irreversible decisions in a visual perception experiment

To examine how amendable decision theory applies in a real-world example, we performed a human visual perception experiment. Participants were asked to observe the motion of a randomly moving dot on a screen, and assess whether the motion was biased towards the left or right direction by pressing a key, see Fig. 3A. In the irrevocable version of the task, pressing a key terminated the game. In the amendable version, participants could alter their decision an arbitrary number of times, until a time limit $t_{\mathrm{f}} = 10$s. At the initial time, the tentative decision $d(t)$ was randomly initialized to + or − with equal probabilities. Both in the irrevocable and amendable version, participants played four different versions of the games of increasing difficulty, i.e., reduced bias. Participants were instructed to decide as fast as possible, but without making too many mistakes.

In keeping with the literature (*6*), we model evidence accumulation as a drift-diffusion process. We consider both an optimal (normative) model (*41*) in which we set the evidence rate to its optimal value ($\gamma = \gamma_{\mathrm{opt}}$) and a descriptive model in which we infer γ from the experimental data. The optimal evidence rate is determined by the drift and diffusion coefficients of the moving dot. Therefore, the optimal amendable decision model has no fitting parameters. In contrast, the optimal irrevocable decision model includes the threshold ℓ as a free parameter.

As predicted by the optimal model, participants were able to make error-free amendable decisions, at least when the task was not too difficult (Fig. 3B). In the hardest version of the game, errors took place. This can be explained within the optimal theory due to the finite duration of each trial (see Fig. 2C and Methods). In contrast, irrevocable decisions were error-prone for all game difficulties, and characterized by a speed-error tradeoff (Fig. 3B).

We now compare the empirical distributions of decision times with those of the optimal drift-diffusion model. For easy games, the empirical distributions present a "gap" for short times (on the order of 0.1s) compared with the theoretical prediction, see Fig. 3C and Fig. 3D. This discrepancy is likely due to the finite response time of players. The tails of the distributions are instead in quantitative agreement with the theoretical ones. For harder games, we find an excellent agreement between the theory and the experiment for all times. This is consistent with the observation that the empirical drift is close to the optimal ones for these games, suggesting that players adopt a nearly optimal strategy. This result could be, again, due to the fact that harder games involve longer decision times, making individual reaction time less of a limiting factor. Empirical decision times distributions for irrevocable games are qualitatively different than those for amendable ones, with a distinct peak at intermediate times for irrevocable decisions, as predicted by the theory (Fig. 3D).

For the descriptive model, we used the experimental data to estimate the evidence rate γ for each participant and each game, see Fig. 4. In the present experiment, in most cases, evidence rates are higher in amendable than in irrevocable games (see Fig. 4), and therefore closer to the optimal ones. This suggests that amendable decision tasks capture the rate of acquired information with higher accuracy than irrevocable tasks. Furthermore, for each of the games, tradeoffs curves calculated for the evidence rate averaged over the participants are in good agreement with participants performance

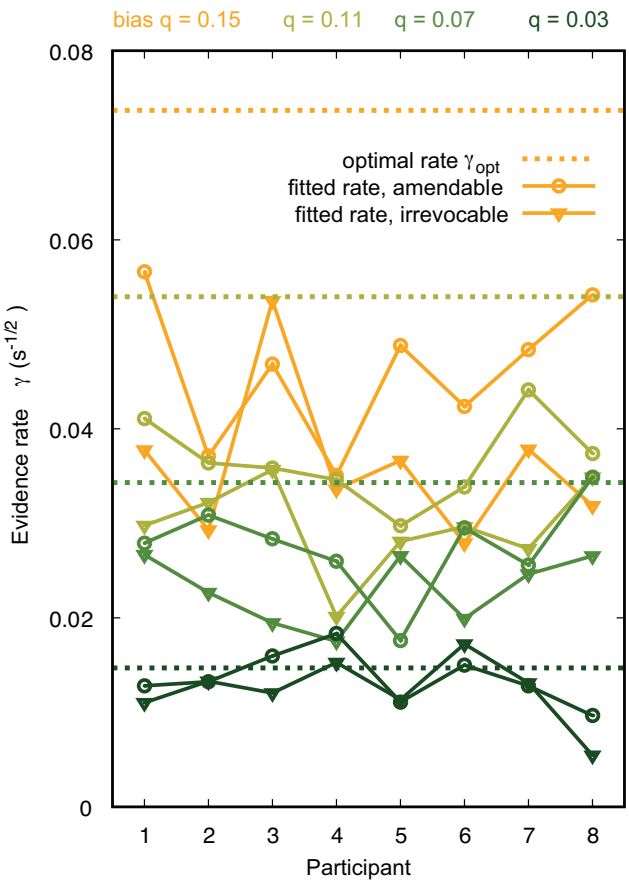

Figure 4: Estimated rates of evidence acquisition γ for the eight participants and the four game difficulties (markers) in the visual perception experiment of Fig. 3 are compared with the optimal evidence rates $\gamma_{\rm opt} = 1/(2\sqrt{\tau})$ (dotted lines) with $\tau = \Delta t/(16q^2)$ (see Methods). As expected, most of the empirical data points lie below the corresponding optimal lines (91% of data points, exceptions are participant 8 in the amendable game with $q = 0.07$, participants 4 and 6 for the irrevocable game with $q = 0.03$, and participants 3, 4 and 6 for the amendable game with $q = 0.03$). In most of the cases, participants displayed a higher evidence rate for amendable than irrevocable games (81% of data points, exceptions are participant 3 for $q = 0.15$, participant 5 for $q = 0.07$, and participants 2, 5, 6, and 7 for $q = 0.03$). For amendable games, the evidence rates are estimated from $\gamma = 1/\sqrt{\langle T_{\rm am}\rangle}$, with $\langle T_{\rm am}\rangle$ the empirically measured value of the mean decision time for each game difficulty. For the hardest game $q = 0.03$, we used theoretical expressions for $\langle T_{\rm am}\rangle$ and η at finite time (see Methods). For irrevocable games, the evidence rates are estimated from the data as described in Methods.

(dashed lines in Fig. 3B).

Amendable decisions in cellular sensing

Biological cells often need to accurately measure the concentration of certain molecules, for example, extracellular ligands or nuclear transcription factors, and make decisions depending on the outcome of the measurement process. These decisions can be conceptualized within our

framework, with the "observer" being the component of the cell responsible for detecting the molecules. In keeping with the literature (*30, 42*), we model the observer as a spherical body that absorbs molecules present in a surrounding fluid at a certain concentration c_∞ far from itself, see Fig. 5A. We assume that the environment is at thermodynamic equilibrium, so that the stationary current of absorbed molecules is given by $j = 4\pi r D c_\infty$, where r is the radius of the observer and D the molecular diffusion coefficient (*30*). The observer's task is to distinguish between two values of the concentration, c_+ and c_-, with $c_+ > c_-$, corresponding to two different rates of incoming molecules, j_+ and j_-, respectively. The number of molecules $N_\pm(t)$ absorbed up to time t represents our observation process. The precision parameter $\epsilon = (c_+ - c_-)/c_+$ quantifies the relative difference between the two concentrations, and therefore the difficulty of the discrimination task.

Also in this case, the optimal choice of the evidence is given by the logarithm of the likelihood ratio process (*11*), which evolves in time according to

$$\frac{dE}{dt} = -\frac{\epsilon}{\tau} + \ln\left(\frac{1}{1-\epsilon}\right)\frac{dN_\pm}{dt}\,, \tag{4}$$

see Methods and (*27*). Here, $\tau = 1/j_+$ is the characteristic time scale.

We compare the average decision times for amendable decisions, irrevocable decisions, and the Berg-Purcell prediction (*30*), see Fig. 5B. In all three cases, the average decision time scales as ϵ^{-2} (see Methods). Amendable decisions are error-free and about a factor two faster than the Berg-Purcell prediction. The average irrevocable decision time depends on the chosen error probability and is, as in the drift-diffusion model, larger than the amendable one for $\eta < 0.08$, approximately (see Methods). In summary, optimal amendable decisions in molecular recognition are error-free and faster than irrevocable decisions models, independently of the difficulty ϵ of the discrimination task.

Mathematical analyses of receptor models often approximate the input signal as a drift-diffusion process (*27*). For amendable decisions, we compute the distribution of decision times without resorting to such approximation (see Methods). The solution shows how the discrete nature of the information obtained from incoming molecules affects the statistics of the decision time. The distribution of decision times is discontinuous, and markedly different depending on whether the plus or minus hypothesis holds. In particular, for the positive hypothesis (higher concentration), the distribution presents a sawtooth shape (Fig. 5C). In contrast, for the negative hypothesis, the distribution is nonzero only over a discrete set of times (Fig. 5D). This difference is due to an asymmetry in the evidence dynamics embodied in (4): the evidence increases in discrete steps whenever the observer absorbs a molecule, while declining continuously in time. In particular, in the negative hypothesis case, each of the discrete decision times corresponds to a given number of molecules absorbed before the decision, see SI (Section 6).

We consider how an amendable concentration test could be implemented biochemically. Ref. (*27*) showed that the evidence dynamics of (17) can be encoded in the concentration ratio of two enzymes: one that decays when ligands are bound and another that decays when molecules are unbound. In the irrevocable case, Ref. (*27*) proposed coupling these enzymes to two downstream Goldbeter-Koshland (GK) modules, that respresent the decision process. Each module acts as a biochemical switch implementing one of the decision thresholds. Importantly, GK modules are reversible switches, and therefore naturally suited to implement amendable decisions as well. Indeed, we find that the amendable concentration test can be biochemically implemented by two decaying enzymes (encoding the evidence dynamics) coupled downstream to a single GK module,

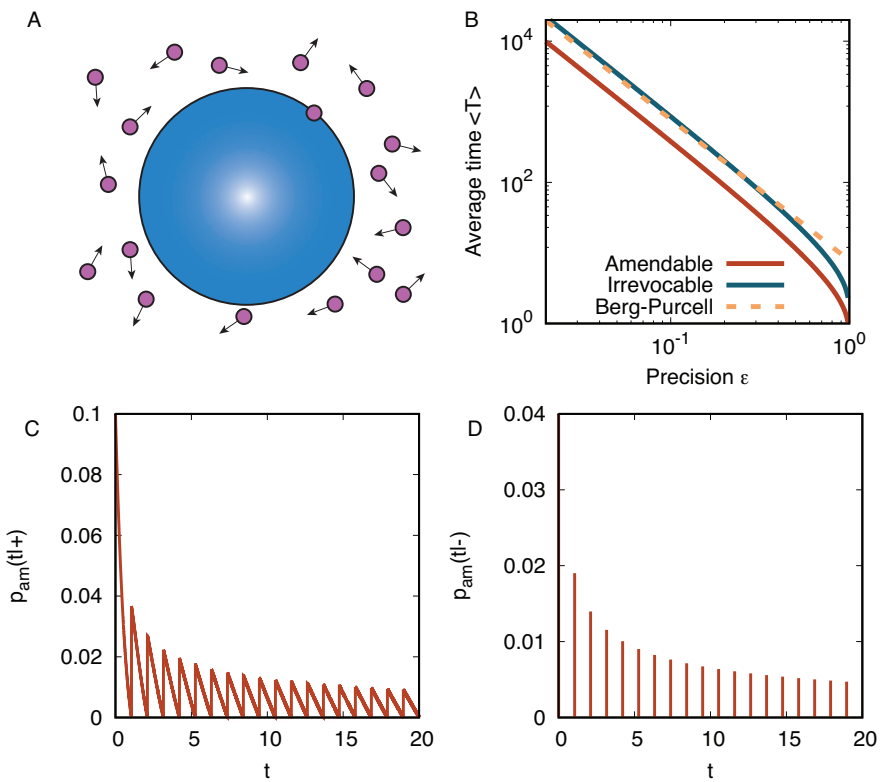

Figure 5: Decisions in molecular sensing. (A) A microscopic observer absorbs molecules from the environment attempting to detect their concentration. (B) Average decision times as a function of the precision ϵ. We have set $\tau = 1$. The Berg-Purcell line is the estimate $\langle T \rangle = (4\pi/(1.61))\epsilon^{-2}$ for the mean decision time that is based on the root mean square fractional error of the concentration, see Eq. (30) in (*30*). For irrevocable decisions we have set $\eta = 0.01$. (C) Distribution of amendable decision times for the + hypothesis and $\epsilon = 0.1$. (D) Same as (C), but for the − hypothesis. The distribution is discrete in this case (see Methods).

which reversibly switches when the evidence $E(t)$ crosses zero (see SI, Section 8). Our model demonstrates that biochemical implementation of amendable decisions is feasible and, at least in this example, requires a simpler reaction network than irrevocable decisions.

Amendable model predicts Hunchback expression profile in Drosophila embryos

Expression of Hunchback represents the first major cell-fate decision made by nuclei in Drosophila embryos, triggered by positional information from the Bicoid gradient (*26*). During the nuclear cycles 9 to 13 of the fruit fly development, the transcription factor Bicoid forms an exponentially decaying expression profile along the anterior-posterior axis of the embryo (*8,29,43,44*). Hunchback is a gene activated by Bicoid that develops an approximately on-off expression profile depending on whether nuclei are situated in the anterior or posterior half of the embryo, respectively (*43–46*), see Fig. 6A. Live imaging of nascent RNA transcription reveals that nuclei in the posterior half sometimes switch off Hunchback expression following a transient activation (*34,35,47*), supporting

the idea of an amendable decision dynamics.

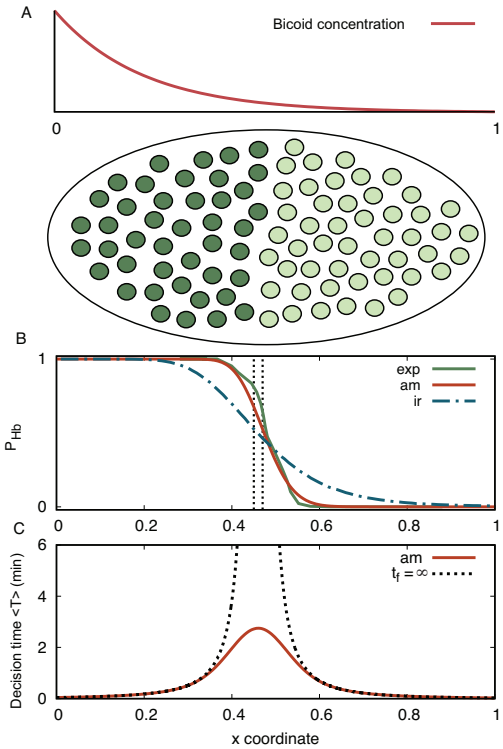

Figure 6: Amendable decisions in the Bicoid-Hunchback system of *Drosophila* embryos. (A) Bicoid is a morphogene that forms a longitudinal concentration gradient along the embryo. Nuclei sense the Bicoid concentrations and decide whether to express Hunchback (anterior half, green circles) or not (posterior half, light circles). (B) Probability $P_{\mathrm{H}b}$ to express Hunchback at the end of the 10-th nuclear cycle as a function of the rescaled coordinate x. Mean average decision times for optimal amendable decisions (red solid line), are compared with experimental data (green solid line) and optimal irrevocable decisions (blue dashed dotted line). Parameters are chosen based on experimental observations (see Methods). Experimental data represent the relative number of nuclei that express the Hunchback gene. These nuclei are identified through fluorescent in situ hybridization (data taken from Figure 3 of Ref. (*45*)), which detects Hunchback RNA transcripts that are bound to the nucleus. The two dotted vertical lines mark the separation between two neighboring nuclei at the Hunchback interface. Results for 11th, 12th, and 13th nuclear cycle are qualitatively similar (see SI, Fig. S11). For amendable decisions there are no fitted parameters, while for the irrevocable case we have fitted the decision thresholds to the experimental curve (see SI, Fig. S10). In cases where neither of the thresholds have been reached at the final time, we assumed that cells do not express Hunchback, as in the case in which the negative threshold is reached. (C) Average decision time for amendable decisions based on the optimal evidence process and using the continuous approximation. Results for $t_{\mathrm{f}} = 5.5$min (solid line) are compared with the case $t_{\mathrm{f}} = \infty$ (dotted line).

To apply our theory to this system, we assume that nuclei are optimized for distinguishing the concentration differences experienced by neighboring nuclei at the point along the embryo axis where Hunchback switches its expression (see Fig. 6A and Methods). The optimal amendable

decision model based on this assumption is able to generate a sharp spatial activation profile of the Hunchback gene in a timescale compatible with that of nuclear cycles, see Fig. 6B. The predicted optimal profile is in excellent quantitative agreement with the experimentally measured one (*45*) without fitting parameters, supporting that the Bicoid-Hunchback system operates in an optimal way. In contrast, the optimal model based on irrevocable decisions leads to a shallower profile that is incompatible with the experiments, regardless of the choice of the decision thresholds (Fig. 6C). The predicted optimal decision times are in the order of minutes, and decrease with the distance from the boundary (Fig. 6D), in qualitative agreement with experiments (*47*) (see SI, Section 8).

It is natural to wonder whether reliable amendable decisions regarding gene transcription can be implemented in individual nuclei. To address this, we developed a biophysical model for amendable decisions in the Bicoid-Hunchback system (see SI, Section 9). In this model, the time-dependent number of Bicoid transcription factors bound to the Hunchback promoter is our observation process $X(t)$. For simplicity, we assume that Bicoid binds independently at the six binding site at the Hunchback promoter (see (*48*)). Following Ref. (*35*), we assume that the promoter stochastically switches between ON and OFF states with rates that depend on $X(t)$. When the promoter is ON, RNA polymerases can initiate transcription; when it is OFF, polymerases stochastically detach from the gene. The evidence process $E(t)$ is taken to be proportional to the length of the longest nascent RNA transcript, minus a constant that accounts for the experimental detection threshold of these transcripts. The decision variable D is set to + if at least one nascent transcript longer than the threshold is present ($E(t) > 0$). Otherwise, we set $D = -$. This model, with biophysically realistic parameters, predicts a decision profile that is sharper than the one for optimal irrevocable decisions, albeit shallower than the optimal amendable one (see SI, Fig. S10). The performance gap with the optimal amendable profile can likely be reduced by parameter optimization. These results demonstrate that evidence-based amendable decision-making is feasible at the level of individual nuclei in early development, and that also in this example amendable decisions yield more reliable outcomes than irrevocable ones.

Discussion

We have shown that amendable decisions are governed by different laws than irrevocable ones. In particular, they can be taken in a finite average time at zero error probability, thereby offering a substantial advantage over irrevocable decisions. Our results challenge the prevailing paradigm in biology that assumes that decisions, once made, cannot be revoked.

We confirmed the difference between amendable and irrevocable decisions in a visual perception experiment, inspired to classic studies (*6, 49*). Our experiment confirmed the possibility of error-free amendable decisions in a finite time as predicted by the theory. The amendable decision model provides an alternative approach for estimating the evidence acquisition rate. This quantity, usually estimated using irrevocable decision tasks (*6*), is important in behavioral psychology to measure the impact of factors such as aging (*50, 51*), aphasia (*52*), and attention-deficit hyperactivity disorder (*53*) on cognitive decline. Our study also paves the way for rationalizing amendable decision behavior in more complex cognitive tasks, such as brightness discrimination (*54*).

Our theory also applies to the microscopic world of cell-fate decisions. For the Bicoid-Hunchback model system, we have shown that the optimal amendable decision model predicts a decision profile along the embryo in excellent quantitative agreement with experimental data and

without fitted parameters. In contrast, the optimal irrevocable model requires setting thresholds, and predicts a shallow decision profile that does not match the experiments. Previous studies have observed that the Bicoid-Hunchback system operates close to the optimal physical limit (*8*), see also (*55*). Our normative theory corroborates this view, and additionally suggests that this limit is reached by an amendable decision process. In biophysical models of the Bicoid-Hunchback model, the steepness of the irrevocable decision profile can be improved by cooperative binding at the Hunchback promoter (*22, 48*). In the amendable case, we have shown that an explicit model of RNA polymerases binding and unbinding provides a simple and biophysically sound mechanism to make accurate decision, even in the absence of cooperative binding.

Our theory can shed light into a broader range of cell-fate decisions, with a particularly exciting potential in the study of cell cycle checkpoints. Cells experiencing severe stress or irreparable DNA damage can arrest their cell cycle. Understanding the conditions underlying these decisions is crucial for cancer biology (*56*). Decisions to delay or arrest the cell cycle are highly dependent on cellular context and history (*57, 58*) and must occur in certain time windows. Cells that have arrested their cycle may re-enter it under certain conditions (*56, 59, 60*). This evidence supports that many cell-fate decisions are amendable. The theoretical framework developed here can reveal whether these decisions are optimally made.

Broader applications of amendable decisions will require going beyond the paradigm of binary hypotheses. Examples are change-point detection problems, of potential relevance for accurate timing of developmental cell-fate decisions (*61*), and multiple hypotheses sequential testing (*13*) for modeling cell differentiation in multicellular organisms.

The superior performance of amendable decisions over irreversible ones begs the question of why certain decision processes in biology are hardly reversed. One way of rationalizing the distinction between amendable and irreversible decisions is to compare the cost of making an error with the cost of correcting it. From this perspective, amendable and irreversible decisions represent two extremes of a continuous spectrum: at one end, the cost of amending a decision is small relative to the cost of making an error; at the other end, the cost of amendment outweighs the consequences of an error. During early development, errors pose a particularly severe risk due to error amplification (*26*), suggesting that amendable decisions may serve as a natural control mechanism.

Materials and Methods

Drift-diffusion: irrevocable decisions

We here present general mathematical results for the drift-diffusion model. We assume that the evidence is a linear function of the observation process X, and thus, for a given hypothesis, obeys the dynamics

$$\frac{dE}{dt} = a + b\,\xi(t), \tag{5}$$

where a and b are constants that depend on which of the two hypotheses holds. We note that (5) is more general than (2) , as the latter assumes that the average evidence rate is odd under switching hypothesis. This assumption always holds at optimality (as we prove in the SI, Section 1). This assumption can also be justified in non-optimal cases when the the two hypothesis are related by a change of sign, $\mu_+ = -\mu_-$, as in our visual perception experiment.

We focus on equally likely hypotheses, so that $E(0) = 0$; the more general case of a nonuniform prior is presented in the SI (Section 2). We start by summarizing known results in the irrevocable case. We assume symmetric thresholds, $\ell_+ = \ell_- = \ell$. The probabilities of reaching the + and − thresholds are

$$p_+ = \frac{e^{\alpha\ell}}{1+e^{\alpha\ell}} \qquad \text{and} \qquad p_- = \frac{1}{1+e^{\alpha\ell}}\,, \tag{6}$$

where $\alpha = 2a/b^2$. This result follows readily from applying Doob's optional stopping theorem to the martingale $M(t) = \exp(-\alpha E(t))$ is a martingale (*62–64*). The error probability η is the sum of the probabilities of false positives and false negatives:

$$\eta = \frac{p_+(H=-) + p_-(H=+)}{2}. \tag{7}$$

The threshold ℓ is often chosen according to the desired value of the error probability. For example, in the case of (2), (6) leads to

$$\ell = \frac{1}{2\gamma}\log\left(\frac{1-\eta}{\eta}\right)\,. \tag{8}$$

The distribution $p_{\rm ir}(t)$ of first-passage times can be obtained from the backward Kolmogorov equation (*65*):

$$p_{\rm ir}(t) = \frac{\pi b^2}{2\ell^2}\cosh\left(\frac{a\ell}{b^2}\right)\sum_{n=0}^{\infty}(-1)^n(2n+1)e^{-\frac{(2n+1)^2\pi^2 b^2 t}{8\ell^2}-\frac{a^2 t}{2b^2}}. \tag{9}$$

Integrating over time, we find for the average decision time

$$\langle T_{\rm ir}\rangle = \frac{\ell(p_+ - p_-)}{a} = \frac{(1-2\eta)}{8\gamma^2}\log\left(\frac{\eta}{1-\eta}\right). \tag{10}$$

The first equality in (10) is a version of Wald's celebrated equation (*66, 67*), while the second equality follows from the Eqs. (6) and (8). Equation (10) leads to the speed-accuracy tradeoff relation $\langle T_{\rm ir}\rangle \sim -\ln(\eta)$, valid for small η. Results for the optimal irrevocable decision strategy, where the evidence process is proportional to the logarithm of the likelihood ratio, are recovered by setting $a = \pm\gamma_{\rm opt} = \pm 1/(2\sqrt{\tau})$ and $b = 1$ in the equations of this section.

Drift-diffusion: amendable decisions

In the amendable case, the decision time is defined as the last time that the evidence E has changed sign. We directly consider the general case in which the evidence is governed by (5) and decisions are taken within a finite time window $[0, t_{\rm f}]$. We denote by $S(\epsilon_E, t)$ the probability that the process, starting from $E = \epsilon_E$ at time 0, does not reach $E = 0$ by time t. This probability is expressed by

$$\begin{aligned} S(\epsilon_E, t) = 1 &- \frac{1}{2}\left[1 - \mathrm{erf}\left(\frac{|\epsilon_E|}{\sqrt{2b^2 t}} + \frac{a\epsilon_E\sqrt{t}}{\sqrt{2}b|\epsilon_E|}\right)\right] \\ &- \frac{e^{-2a\epsilon_E/b^2}}{2}\left[1 - \mathrm{erf}\left(\frac{|\epsilon_E|}{\sqrt{2b^2 t}} - \frac{a\epsilon_E\sqrt{t}}{\sqrt{2}b|\epsilon_E|}\right)\right]\,, \end{aligned} \tag{11}$$

where $\mathrm{erf}(x) = (2/\sqrt{\pi}) \int_0^x e^{-t^2}\, \mathrm{d}t$ is the error function, see, e.g., Section (3.2.2) in Ref. (*39*). If ϵ_E is small, starting from $E = 0$ a fluctuation leads to $E = \epsilon_E$ or $E - \epsilon_E$ with equal probability due to the properties of Brownian motion. Thus, the escape probability takes the form

$$\begin{aligned} s(t) &= \lim_{\epsilon_E \to 0^+} \frac{S(\epsilon_E, t) + S(-\epsilon_E, t)}{2\epsilon_E} \\ &= \frac{a}{b^2} \mathrm{erf}\left(\frac{a\sqrt{t}}{\sqrt{2}b}\right) + \sqrt{\frac{2}{\pi b^2 t}} e^{-a^2 t/(2b^2)}. \end{aligned} \tag{12}$$

The finite-time decision time distribution is proportional to the probability of being in state $E = 0$ at time t, times the probability that the process will not return to the state $E = 0$ by time t_{t_f}, viz.,

$$p_\mathrm{am}(t|t_\mathrm{f}) = b^2 \frac{e^{-\frac{a^2 t}{2b^2}}}{\sqrt{2\pi b^2 t}} s(t_\mathrm{f} - t)\,, \tag{13}$$

where the prefactor b^2 can be either justified by a dimensional argument, or by numerically verifying the normalization condition.

At finite times, amendable decisions entail a finite error probability. If the decision process is reliable, then this probability is simply given by the probability that, at the final time, the sign of the evidence E is different than the sign of the bias a. Since the distribution of E is Gaussian at any time, we find

$$\eta = \frac{1}{2} - \frac{1}{2} \mathrm{erf}\left(\frac{a t_\mathrm{f}}{\sqrt{2b^2 t_\mathrm{f}}}\right). \tag{14}$$

In the limit $t_\mathrm{f} \to \infty$, we obtain the infinite time results mentioned in the Results, i.e., a vanishing error probability and a distribution of decision times given by

$$p_\mathrm{am}(t) = \frac{|a|}{\sqrt{2\pi b^2 t}} \exp\left(-\frac{a^2 t}{2b^2}\right). \tag{15}$$

Notice that for $a = 0$ (13) reduces to $p_\mathrm{am}(t|E_0, t_\mathrm{f}) = 1/[\pi\sqrt{t(t - t_\mathrm{f})}]$, which is the second arcsine law for Brownian motion (*68*). The corresponding average decision time is expressed by

$$\langle T_\mathrm{am} \rangle = \frac{b^2}{a^2}. \tag{16}$$

The optimal decision strategy, which corresponds with evidence processes that are proportional to the logarithm of the likelihood ratio process (see SI, Section 1), is recovered by setting $a = \pm\gamma_\mathrm{opt} = \pm 1/(2\sqrt{\tau})$ and $b = 1$.

Visual perception experiment: protocol

Eight volunteering participants were selected among students and researchers at OIST. Each participant repeatedly played a game in which a dot randomly moves on a computer screen, with the goal to assess whether the motion was biased towards the left or right direction and make decisions using the computer keyboard.

The game had an irrevocable and amendable version. In the irrevocable version, the game ended once a decision was taken, while in the amendable version participants could alter their decision an arbitrary number of times, up to a time limit of 10s. For both types of games, participants were asked to decide rapidly while avoiding mistakes.

Each participant played eight groups of 30 games each. Four out of eight groups consisted of irrevocable games and the remaining four of amendable games. Irrevocable and amendable groups of games were played in an alternate fashion. Half of the participants started with an irrevocable group and half with an amendable group, to remove potential biases. The four groups for each game involved an increasing level of difficulty. Specifically, we express as $(1/2 + q)$ and $(1/2 - q)$ the probabilities of moving in the direction of the bias or in the opposite direction, respectively, during a timestep $\Delta t = (1/60)$s of the game. The bias parameter q ranged in the set of values $q \in (0.15, 0.11, 0.07, 0.03)$ for the four games. The corresponding parameters of the observation process are $\mu_\pm = \pm 2q/\Delta t$ and $\sigma^2 = 1/\Delta t$. The dot also performed unbiased Brownian motion in the vertical direction.

Each of the 8 participant performed the experiment in a single session. Participants were asked to read an instruction sheet outlining the description of the amendable and irrevocable games. The instruction sheet also included a consent agreement. Participants were then given an opportunity to ask questions to clarify possible doubts. All participants provided informed consent.

Before the actual experiment, participants had the opportunity to practice both irrevocable and amendable games. They first could practice these games in a simplified version, in which the initial position of the dot was marked with a vertical dashed line. They then could practice the normal version of the game, without the reference line. For all the practice games, the difficulty was set to $q = 0.07$. Each version of the practice game could be played for as long as the participants felt comfortable with. Both in the practice and actual experiment, the game provided summary information at the end of each round, such as whether the decision was correct or incorrect, the decision time, and the average decision time. During the actual experiment, participants were encouraged to take breaks of a few minutes between the $4 \times 2 = 8$ groups of games. The entire session lasted about one hour per participant, including the introduction and practice.

Participants were anonymized before the data analysis. The study protocol was approved by the OIST human subject research committee (reference number HSR-2024-016-2).

Visual perception experiment: data analysis

In the optimal (normative) model, we obtain the evidence rate from the drift and diffusion coefficients characterizing the dot motion: $\gamma = \gamma_{\text{opt}} = 2q/\sqrt{\Delta t}$. This parameter fully specifies the optimal amendable model. For the optimal irrevocable model, we estimate the decision threshold ℓ from the average empirical error probability through (8).

In the descriptive model, the evidence rate is estimated from the experimental data. This estimate is different in the amendable and irrevocable cases. For amendable decisions, we combine (16) and (2), obtaining $\gamma = 1/\sqrt{\langle T_{\text{am}} \rangle}$. This formula permits to simply estimate the evidence rate from the average decision time. For the hardest game ($q = 0.03$), we took finite-time effects into account to estimate the drift. This can be done either from the mean decision time (obtained by numerically integrating (13)) or from the error probability, (14). To be conservative, we took the smallest of these two values for each point. In the irrevocable case, we estimate the evidence rate by solving

the expression of $\langle T_{\rm ir}\rangle$ and η towards γ and ℓ. This procedure leads to $\gamma = \sqrt{\phi \tanh[\phi/2]/(2\langle T_{\rm ir}\rangle)}$ and $\ell = \sqrt{\phi\langle T_{\rm ir}\rangle/[2\tanh(\phi/2)]}$, where $\phi = \log[\eta/(1-\eta)]$.

Cellular sensing model

Our starting point is the equation governing the evidence

$$\frac{dE}{dt} = (j_- - j_+) + \ln\left(\frac{j_+}{j_-}\right)\frac{dN_\pm(t)}{dt} \tag{17}$$

for $j_+ > j_-$, see (*27*), and the initial condition $E_0 = 0$. Expressing j_- and j_+ in terms of the precision parameter ϵ and the characteristic time scale τ directly leads to (4).

We study the amendable decision time distribution for $t_f = \infty$. The decision time is the last time when the sign of the evidence was inconsistent with the hypothesis, i.e., $\text{sign}(E(t)) = -H$. For $H = +$, we find

$$p_{\rm am}(t|H=+) = j_+(1 - e^{-\Delta(n+1-t/\tau_{\rm r})})e^{-j_+t}\frac{(j_+t)^n}{n!}\,, \tag{18}$$

where $\Delta = \ln j_+/j_- = \ln(1/[1-\epsilon])$, $\tau_{\rm r} = (\tau/\epsilon)\Delta$, and $t \in [n\tau_{\rm r}, (n+1)\tau_{\rm r}]$ (see SI, Section 6). For the negative hypothesis, we obtain

$$p_{\rm am}(t|H=-) = (1 - j_-\tau_{\rm r})\sum_{n=0}^{\infty} e^{-j_-t}\frac{(j_-t)^n}{n!}\delta\left(t - \tau_{\rm r}n\right)\,. \tag{19}$$

The average decision time for the negative hypothesis is expressed by

$$\langle T_{\rm am}|H=-\rangle = \frac{j_-\tau_{\rm r}^2}{(1-j_-\tau_{\rm r})^2}. \tag{20}$$

For the positive hypothesis, we could not find a simple expression for the average decision time. Nevertheless, this time can be obtained from numerically integrating (18). Alternatively, one can use a diffusion approximation of the counting process:

$$\frac{dN_\pm}{dt} \approx j_\pm + \sqrt{j_\pm}\xi(t)\,. \tag{21}$$

Using (16), we then find

$$\langle T_{\rm am}|H=\pm\rangle = \frac{j_\pm \ln^2(1-\epsilon)}{[j_\pm\ln(1-\epsilon) + \epsilon/\tau]^2}. \tag{22}$$

We note that, for the negative hypothesis, the continuous approximation of (22) exactly matches the solution given in (20). In contrast, for the positive hypothesis, (22) only approximates the numerically evaluated mean decision time.

To determine the mean irrevocable decision times $\langle T_{\rm irr}|H=\pm\rangle$ for the two hypotheses, we use again Wald's equation (*64, 66, 67*)

$$\begin{aligned}\langle T_{\rm irr}|H=\pm\rangle = &\left\langle \frac{dE}{dt}\Big|H=\pm\right\rangle \\ &\times\left(p_+\langle E(T)|D=+\rangle + p_-\langle E(T)|D=-\rangle\right)\end{aligned} \tag{23}$$

where

$$\left\langle \frac{dE}{dt} \middle| H = \pm \right\rangle = -\frac{\epsilon}{\tau} + j_{\pm} \ln \frac{1}{1-\epsilon}\,, \tag{24}$$

and where we set

$$\langle E(T)|D = +\rangle = \ell_+ \quad \text{and} \quad \langle E(T)|D = -\rangle = -\ell_-, \tag{25}$$

neglecting overshoots. We have verified with simulations that neglecting overshoots yields a very good approximation.

Averaging (22) and (23) over the two hypotheses and taking the ratio of the two times, we find that this ratio is independent of the precision ϵ:

$$\frac{\langle T\rangle_{\text{ir}}}{\langle T\rangle_{\text{am}}} \approx \frac{(1-2\eta)}{2} \ln\left(\frac{1}{\eta} - 1\right)\,. \tag{26}$$

Bicoid-Hunchback model

We describe the Bicoid concentration gradient as

$$c(x) = c_0\, e^{-\lambda(x - x_{\text{m}})}, \tag{27}$$

see (*8, 29, 43*), where $x \in [0, 1]$ denotes the relative position along the anterior-posterior axis ($x = 0$ is the anterior pole and $x = 1$ the posterior pole, corresponding to about $500\mu m$), $\lambda = 5$ is the inverse of the decay length of the concentration profile and $c_0 = 4.8 \pm 0.6\mu m^{-3}$ is the Bicoid concentration at the mid point x_m where the Hunchback profile switches from high to low ($x_m \approx 0.45$ for the 10-th nuclear cycle (*8, 45*)). We estimate the distance between neighboring nuclei as $\Delta x = 0.02$.

Due to the reproducibility of the midpoint x_m across embryos, and due to the sharp decline of the Hunchback expression profile at the midpoint, we assume that the two hypotheses correspond to two Bicoid concentrations close to the Hunchback boundary, separated by one nucleus diameter: $c_+ = c(x_{\text{m}})$ and $c_- = c(x_{\text{m}} + \Delta x)$. This choice corresponds to a precision $\epsilon = (c_+ - c_-)/c_+ = 0.1$ and a timescale $\tau = 20\,\text{s}$. Our model is then expressed by

$$\frac{dE(x,t)}{dt} = -\frac{\epsilon}{\tau} + \ln\left(\frac{1}{1-\epsilon}\right) \frac{dN(x,t)}{dt}\,, \tag{28}$$

see (4), where $N(x,t)$ is a Poisson point process in t of rate $j(x) = 4\pi r D c(x)$, representing the rate at which Bicoid molecules hit the Hunchback promotor at position x. Following Ref. (*29*), we take $D = 0.3(\mu m)^2/s$ (but see (*69*)) and $r = 3\text{nm}$.

We consider the model dynamics up to a finite time $t_{\text{f}} = 5.5$ min, representing the time that a discrete nuclear envelope is observed during nuclear cycle 10, see Table 1 in Ref. (*70*). The reason is the nuclear envelope breaks down, so that the Bicoid concentration drastically decreases, at the end of each cycle (*29*).

The probability p_{Hb} to express Hunchback is given by the probability that the evidence process is positive at time t_{f}. Using that $N(x,t)$ is a Poisson random variable, we obtain

$$p_{\text{Hb}}(x) = 1 - e^{-t_{\text{f}} j(x)} \sum_{n=0}^{n_{t_{\text{f}}}} \frac{(t_{\text{f}} j(x))^n}{n!}\,, \tag{29}$$

with $n_{t_{\text{f}}} = \lfloor t_{\text{f}}(j_+ - j_-)/\ln(j_+/j_-) \rfloor$ and $\lfloor \cdot \rfloor$ representing the floor function.

Acknowledgements

IN conducted part of this research while visiting the Okinawa Institute of Science and Technology (OIST) through the Theoretical Sciences Visiting Program (TSVP). We thank A. Sassi for assistance with the visual perception experiment. We thank E. Kanemoto and G. Tripp for feedback on the experimental protocol, H. Sprekeler for comments on the drift-diffusion model, and S. Bo, N. Luscombe, and G. Tkacik for feedback on a preliminary version of the manuscript.

References and Notes

1. L. Chittka, P. Skorupski, N. E. Raine, Speed–accuracy tradeoffs in animal decision making. *Trends in ecology & evolution* **24** (7), 400–407 (2009).

2. P. R. Backwell, N. I. Passmore, Time constraints and multiple choice criteria in the sampling behaviour and mate choice of the fiddler crab, Uca annulipes. *Behavioral Ecology and Sociobiology* **38**, 407–416 (1996).

3. L. Chittka, A. G. Dyer, F. Bock, A. Dornhaus, Bees trade off foraging speed for accuracy. *Nature* **424** (6947), 388–388 (2003).

4. H. MaBouDi, J. A. Marshall, N. Dearden, A. B. Barron, How honey bees make fast and accurate decisions. *Elife* **12**, e86176 (2023).

5. L. Chittka, D. Osorio, Cognitive dimensions of predator responses to imperfect mimicry. *PLoS Biology* **5** (12), e339 (2007).

6. R. Ratcliff, G. McKoon, The diffusion decision model: theory and data for two-choice decision tasks. *Neural computation* **20** (4), 873–922 (2008).

7. D. Rinberg, A. Koulakov, A. Gelperin, Speed-accuracy tradeoff in olfaction. *Neuron* **51** (3), 351–358 (2006).

8. T. Gregor, D. W. Tank, E. F. Wieschaus, W. Bialek, Probing the limits to positional information. *Cell* **130** (1), 153–164 (2007).

9. W. Bialek, *Biophysics: searching for principles* (Princeton University Press) (2012).

10. S. Kira, T. Yang, M. N. Shadlen, A neural implementation of Wald's sequential probability ratio test. *Neuron* **85** (4), 861–873 (2015).

11. A. Wald, Sequential tests of statistical hypotheses. *Ann. Math. Statist.* **16** (2), 117–186 (1945).

12. J. L. Melsa, D. L. Cohn, *Decision and estimation theory* (McGraw-Hill) (1978).

13. A. Tartakovsky, I. Nikiforov, M. Basseville, *Sequential analysis: Hypothesis testing and change-point detection*, vol. 136 of *Monographs on statistics and applied probability* (CRC press) (2015).

14. J. I. Gold, M. N. Shadlen, The neural basis of decision making. *Annu. Rev. Neurosci.* **30** (1), 535–574 (2007).

15. N. Uchida, A. Kepecs, Z. F. Mainen, Seeing at a glance, smelling in a whiff: rapid forms of perceptual decision making. *Nature Reviews Neuroscience* **7** (6), 485–491 (2006).

16. R. Bogacz, E.-J. Wagenmakers, B. U. Forstmann, S. Nieuwenhuis, The neural basis of the speed–accuracy tradeoff. *Trends in neurosciences* **33** (1), 10–16 (2010).

17. H. Kaneko, H. Tamura, T. Kawashima, S. S. Suzuki, A choice reaction-time task in the rat: a new model using air-puff stimuli and lever-release responses. *Behavioural brain research* **174** (1), 151–159 (2006).

18. N. Stroeymeyt, M. Giurfa, N. R. Franks, Improving decision speed, accuracy and group cohesion through early information gathering in house-hunting ants. *PLoS one* **5** (9), e13059 (2010).

19. L. Wolpert, Positional information and the spatial pattern of cellular differentiation. *Journal of theoretical biology* **25** (1), 1–47 (1969).

20. H. L. Ashe, J. Briscoe, The interpretation of morphogen gradients. *Development* **133**, 385–394 (2006).

21. M. Ibanes, J. C. I. Belmonte, Theoretical and experimental approaches to understand morphogen gradients. *Molecular Systems Biology* **4** (1), 176 (2008).

22. J. Desponds, M. Vergassola, A. M. Walczak, A mechanism for hunchback promoters to readout morphogenetic positional information in less than a minute. *Elife* **9**, e49758 (2020).

23. P. François, G. Voisinne, E. D. Siggia, G. Altan-Bonnet, M. Vergassola, Phenotypic model for early T-cell activation displaying sensitivity, specificity, and antagonism. *Proceedings of the National Academy of Sciences* **110** (10), E888–E897 (2013).

24. C. Li, J. Wang, Quantifying cell fate decisions for differentiation and reprogramming of a human stem cell network: landscape and biological paths. *PLoS computational biology* **9** (8), e1003165 (2013).

25. T. J. Kobayashi, Implementation of dynamic Bayesian decision making by intracellular kinetics. *Physical review letters* **104** (22), 228104 (2010).

26. G. Balázsi, A. Van Oudenaarden, J. J. Collins, Cellular decision making and biological noise: from microbes to mammals. *Cell* **144** (6), 910–925 (2011).

27. E. D. Siggia, M. Vergassola, Decisions on the fly in cellular sensory systems. *Proceedings of the National Academy of Sciences* **110** (39), E3704–E3712 (2013).

28. T. Tohme, M. Vergassola, T. Mora, A. M. Walczak, Fast decisions with biophysically constrained gene promoter architectures. *arXiv preprint arXiv:2507.03720* (2025).

29. T. Gregor, E. F. Wieschaus, A. P. McGregor, W. Bialek, D. W. Tank, Stability and nuclear dynamics of the bicoid morphogen gradient. *Cell* **130** (1), 141–152 (2007).

30. H. C. Berg, E. M. Purcell, Physics of chemoreception. *Biophysical journal* **20** (2), 193–219 (1977).

31. A. Resulaj, R. Kiani, D. M. Wolpert, M. N. Shadlen, Changes of mind in decision-making. *Nature* **461** (7261), 263–266 (2009).

32. R. van Den Berg, *et al.*, A common mechanism underlies changes of mind about decisions and confidence. *Elife* **5**, e12192 (2016).

33. C. Stone, J. B. Mattingley, D. Rangelov, On second thoughts: changes of mind in decision-making. *Trends in Cognitive Sciences* **26** (5), 419–431 (2022).

34. H. G. Garcia, M. Tikhonov, A. Lin, T. Gregor, Quantitative imaging of transcription in living Drosophila embryos links polymerase activity to patterning. *Current biology* **23** (21), 2140–2145 (2013).

35. P.-T. Chen, B. Zoller, M. Levo, T. Gregor, Common bursting relationships underlie eukaryotic transcription dynamics. *arXiv preprint: https://arxiv.org/abs/2304.08770* (2023).

36. S. Huang, G. Eichler, Y. Bar-Yam, D. E. Ingber, Cell fates as high-dimensional attractor states of a complex gene regulatory network. *Physical review letters* **94** (12), 128701 (2005).

37. M. Mojtahedi, *et al.*, Cell fate decision as high-dimensional critical state transition. *PLoS biology* **14** (12), e2000640 (2016).

38. F. Corson, E. D. Siggia, Gene-free methodology for cell fate dynamics during development. *Elife* **6**, e30743 (2017).

39. S. Redner, *A guide to first-passage processes* (Cambridge university press) (2001).

40. A. Wald, J. Wolfowitz, Optimum character of the sequential probability ratio test. *The Annals of Mathematical Statistics* pp. 326–339 (1948).

41. E. J. Johnson, R. Ratcliff, Computational and process models of decision making in psychology and behavioral economics, in *Neuroeconomics*, P. W. Glimcher, E. Fehr, Eds. (Elsevier), chap. 3, pp. 35–47, 2nd ed. (2014).

42. R. G. Endres, N. S. Wingreen, Accuracy of direct gradient sensing by single cells. *Proceedings of the National Academy of Sciences* **105** (41), 15749–15754 (2008).

43. B. Houchmandzadeh, E. Wieschaus, S. Leibler, Establishment of developmental precision and proportions in the early Drosophila embryo. *Nature* **415** (6873), 798–802 (2002).

44. O. Crauk, N. Dostatni, Bicoid determines sharp and precise target gene expression in the Drosophila embryo. *Current Biology* **15** (21), 1888–1898 (2005).

45. A. Porcher, *et al.*, The time to measure positional information: maternal hunchback is required for the synchrony of the Bicoid transcriptional response at the onset of zygotic transcription. *Development* **137** (16), 2795–2804 (2010).

46. G. Tkačik, T. Gregor, The many bits of positional information. *Development* **148** (2), dev176065 (2021).

47. T. Lucas, *et al.*, Live imaging of bicoid-dependent transcription in Drosophila embryos. *Current biology* **23** (21), 2135–2139 (2013).

48. T. Mijatović, A. R. Kok, M. Brüggen, J. W. Zwanikken, M. Bauer, Weak transcription factor clustering at binding sites can facilitate information transfer from molecular signals. *PRX Life* **4** (1), 013003 (2026).

49. X.-J. Wang, Probabilistic decision making by slow reverberation in cortical circuits. *Neuron* **36** (5), 955–968 (2002).

50. R. Ratcliff, A. Thapar, G. McKoon, The effects of aging on reaction time in a signal detection task. *Psychology and aging* **16** (2), 323 (2001).

51. P. Kelber, V. Mittelstädt, R. Ulrich, Interplay of aging and practice in conflict processing: A big-data diffusion-model analysis. *Psychology and Aging* (2024).

52. R. Ratcliff, M. Perea, A. Colangelo, L. Buchanan, A diffusion model account of normal and impaired readers. *Brain and Cognition* **55** (2), 374–382 (2004).

53. N. R. Ging-Jehli, R. Ratcliff, L. E. Arnold, Improving neurocognitive testing using computational psychiatry—A systematic review for ADHD. *Psychological Bulletin* **147** (2), 169 (2021).

54. R. Ratcliff, A diffusion model account of response time and accuracy in a brightness discrimination task: Fitting real data and failing to fit fake but plausible data. *Psychonomic bulletin & review* **9** (2), 278–291 (2002).

55. J. Estrada, F. Wong, A. DePace, J. Gunawardena, Information integration and energy expenditure in gene regulation. *Cell* **166** (1), 234–244 (2016).

56. H. K. Matthews, C. Bertoli, R. A. de Bruin, Cell cycle control in cancer. *Nature reviews Molecular cell biology* **23** (1), 74–88 (2022).

57. V. Rivas, *et al.*, GRK2-mediated AKT activation controls cell cycle progression and G2 checkpoint in a p53-dependent manner. *Cell Death Discovery* **10** (1), 385 (2024).

58. C. Ma, E. Gurkan-Cavusoglu, A comprehensive review of computational cell cycle models in guiding cancer treatment strategies. *NPJ Systems Biology and Applications* **10** (1), 71 (2024).

59. I. A. Shaltiel, L. Krenning, W. Bruinsma, R. H. Medema, The same, only different–DNA damage checkpoints and their reversal throughout the cell cycle. *Journal of cell science* **128** (4), 607–620 (2015).

60. J. A. Cornwell, *et al.*, Loss of CDK4/6 activity in S/G2 phase leads to cell cycle reversal. *Nature* **619** (7969), 363–370 (2023).

61. G. Patil, J. S. van Zon, Timers, variability, and body-wide coordination: C. elegans as a model system for whole-animal developmental timing. *Current Opinion in Genetics & Development* **85**, 102172 (2024).

62. D. Williams, *Probability with martingales* (Cambridge university press) (1991).

63. É. Roldán, *et al.*, Martingales for physicists: a treatise on stochastic thermodynamics and beyond. *Advances in Physics* **72** (1-2), 1–258 (2023).

64. I. Neri, Martingale approach for first-passage problems of time-additive observables in Markov processes. *Journal of Physics A: Mathematical and Theoretical* **58** (14), 145002 (2025).

65. C. W. Gardiner, Handbook of stochastic methods for physics, chemistry and the natural sciences. *Springer series in synergetics* (1985).

66. A. Wald, On cumulative sums of random variables. *The Annals of Mathematical Statistics* **15** (3), 283–296 (1944).

67. A. Dvoretzky, J. Kiefer, J. Wolfowitz, Sequential decision problems for processes with continuous time parameter. Testing hypotheses. *The Annals of Mathematical Statistics* **24** (2), 254–264 (1953).

68. A. C. Barato, É. Roldán, I. A. Martínez, S. Pigolotti, Arcsine laws in stochastic thermodynamics. *Physical review letters* **121** (9), 090601 (2018).

69. A. Abu-Arish, A. Porcher, A. Czerwonka, N. Dostatni, C. Fradin, High mobility of bicoid captured by fluorescence correlation spectroscopy: implication for the rapid establishment of its gradient. *Biophysical journal* **99** (4), L33–L35 (2010).

70. V. E. Foe, B. M. Alberts, Studies of nuclear and cytoplasmic behaviour during the five mitotic cycles that precede gastrulation in Drosophila embryogenesis. *Journal of cell science* **61** (1), 31–70 (1983).